make the exchange rate about 10^5–10^8 times faster, since the axial water molecule exchanges with a rate constant of $\sim 10^8$ s^{-1}.[26] The fact that both $(H_2O)_4(OH)VO^+$ and $(H_2O)_4VO_2^+$[6] react with H_4DFB^+ with approximately equal rate constants (1×10^5 M^{-1} s^{-1} and 2.3×10^5 M^{-1} s^{-1}, respectively) makes this model more attractive than the one involving formation of hydrogen bonds.

It is generally accepted that the inner-sphere substitution reactions proceed via a mechanism in which the formation of an outer-sphere complex precedes the rate-determining step. The formation rate constant is defined as $k_f = k_{ex}K_{out}$, where k_{ex} and K_{out} are the water-exchange rate constant and the outer-sphere complex stability constant, respectively. K_{out} can be calculated according to the Eigen–Fuoss equation[31] for (2+,1+) interaction. However, H_4DFB^+ is a large and nonspherical ion, making an estimation of the closest approach of the reacting species very uncertain and the calculated value of K_{out} unreliable. On the other hand, K_{out} for the $Fe(H_2O)_5OH^{2+}$–H_4DFB^+ outer-sphere complex can be calculated easily as $k_f/k_{ex} = 3.6 \times 10^3/1.2 \times 10^5 = 3 \times 10^{-2}$ M^{-1}.[22,32] Since the hydroxoiron(III) and vanadyl ions are equally charged, their outer-sphere stability constants should not differ significantly. Therefore, this value of K_{out} and k_1 given in Table I can be used for calculation of water-exchange rate constants of vanadyl ion, which then can be compared to the experimental value. The calculated value of $k_{ex} = k_1/K_{out} = 563$ s^{-1} favorably compares to the experimental $k_{ex} = 500$ s^{-1}.[26] This suggests that the substitution of a water molecule by H_4DFB^+ on these two metal ions follows the same dissociative mechanism because their rates appears to be dominated by the water exchange. Unfortunately, a lack of relevant data for the water exchange on $(H_2O)_4VO(OH)^+$ makes a similar analysis for this ion impossible.

Che and Kustin[27] reported a much smaller effect of the hydroxo ligand for the complex formation kinetics of vanadyl ion with a series of bidentate ligands than what we observed for H_4DFB^+. However, it should be noted that the experimental conditions used in these two studies are very different (they worked at pH ranging from 3 to 4.5 but at much higher vanadyl concentrations where dimerization of vanadyl ion cannot be excluded).

The kinetic steps that follow the initial formation of the bidentate complex are faster and were studied only for the hydrolysis of the produced complex. The fastest and kinetically well-resolved step was attributed to the formation of the bidentate complex by the hydrolysis of the tetradentate complex. Even though it is dangerous to compare the kinetics of the asymmetric vanadyl ion with the kinetics of the symmetric Fe(III) ion, the obtained values of the hydrolysis rate constants of the tetradentate-bound complexes of these two metal ions confirm that the assignment of the kinetic step is reasonable. The unwrapping of the ferri tetradentate complex appears to be ca. 50 times slower than that of the analogous vanadyl complex. This is qualitatively what one may expect considering the effect of the coordinated oxo group on the charge of the central metal ion and in turn on the kinetic stability of its desferrioxamine B complex.

Acknowledgment. We thank Prof. R. G. Wilkins for using the rapid-scan facilities at the New Mexico State University and Dr. V. Nöthig-Laslo from the "Rudjer Bošković Institute", Zagreb, for recording the ESR spectra. This work received financial support from the Croatian Fund for Research, which is gratefully acknowledged.

(31) Eigen, M. *Z. Phys. Chem. (Frankfurt)* **1954**, *1*, 176. Fuoss, R. M. *J. Am. Chem. Soc.* **1958**, *80*, 5059.
(32) Swadle, T. W.; Merbach, A. E. *Inorg. Chem.* **1981**, *20*, 4212.

Contribution from the Department of Macromolecular Science, Faculty of Science, Osaka University, Toyonaka, Osaka 560, Japan

Influence of the Distal Para Substituent through NH---S Hydrogen Bonds on the Positive Shift of the Reduction Potentials of $[Fe_4S_4(Z\text{-cys-Gly-NHC}_6H_4\text{-}p\text{-X})_4]^{2-}$ (X = H, OMe, F, Cl, CN) Complexes

Ryotaro Ohno, Norikazu Ueyama, and Akira Nakamura*

Received February 5, 1991

$[Fe_4S_4(Z\text{-cys-Gly-NHC}_6H_4\text{-}p\text{-X})_4]^{2-}$ (X = H, OMe, F, Cl, CN) complexes were prepared as models of *P. aerogenes* ferredoxin, whose redox potential is controlled by NH---S hydrogen bonds. Their reduction potentials became more positive in CH_2Cl_2 at 298 K as the electron-withdrawing tendency of the substituent increased. The most positive potential was observed at −0.80 V vs SCE for the 3−/2− couple of $[Fe_4S_4(Z\text{-cys-Gly-NHC}_6H_4\text{-}p\text{-CN})_4]^{2-}$ (**1**), in which all of the amide NH of an anilide residue participated in intramolecular NH---S hydrogen bonds probably with a cysteinyl sulfur atom. The reduction potential of **1** controlled by the electronic property of its ligand was −1.13 V vs SCE.

Introduction

Ferredoxins have the function of electron transfer and are characterized by a cluster consisting of four iron atoms coordinated by four inorganic sulfide ions and thiolate groups of cysteine residues.[1] One important aspect of ferredoxin research has been the elucidation of controlling factors of the reduction potential.

Holm and his co-workers have extensively investigated the reduction potentials of $(Fe_4S_4)^{2+}$ ferredoxin model complexes with alkane- and arenethiolato ligands and found that not only the dielectric constant of a solvent[2,3] but also the electronic property of a ligand[3] exerted influences on the reduction potentials of $(Fe_4S_4)^{2+}$ complexes. However, reduction potentials of their model complexes were far more negative than those of native ferredoxins.[1]

On the other hand, it has been proposed that NH---S hydrogen bonds are the major mechanism of influence of a polypeptide on reduction potentials of ferredoxins as evidenced by the X-ray analysis of *P. aerogenes* ferredoxin.[4] Actually, we experimentally verified the influence of NH---S hydrogen bonds on the reduction potential using ferredoxin model complexes with tripeptide ligands containing a sequence Cys-Gly-Ala, which was characteristic of *P. aerogenes* ferredoxin.[5] Reduction potentials of $[Fe_4S_4(Z\text{-cys-Gly-Ala-OMe})_4]^{2-}$[6] (Z = benzyloxycarbonyl) and $[Fe_4S_4(Z\text{-cys-Gly-Ala-cys-OMe})_2]^{2-}$ shifted positively in CH_2Cl_2 at low temperature, where NH---S hydrogen bonds from NH of the Ala

(1) Berg, J. M.; Holm, R. H. Iron-Sulfur Proteins. In *Metal Ions in Biology*; Spiro, T. G., Ed.; Wiley-Interscience: New York, 1982; Vol. 4, p 1.
(2) Hill, C. L.; Renaud, J.; Holm, R. H.; Mortenson, L. E. *J. Am. Chem. Soc.* **1977**, *99*, 2549.
(3) DePamphilis, B. V.; Averill, B. A.; Herskovitz, T.; Que, L., Jr.; Holm, R. H. *J. Am. Chem. Soc.* **1974**, *96*, 4159.
(4) Carter, C. W. *J. Biol. Chem.* **1977**, *252*, 7802.
(5) (a) Ueyama, N.; Terakawa, T.; Nakata, M.; Nakamura, A. *J. Am. Chem. Soc.* **1983**, *105*, 7098. (b) Ueyama, N.; Kajiwara, A.; Terakawa, T.; Ueno, T.; Nakamura, A. *Inorg. Chem.* **1985**, *24*, 4700.
(6) Small letter cys represents Cys residue coordinating to Fe ion.

0020-1669/91/1330-4887$02.50/0

residue to S of the Cys residue were partially formed by the conformational freezing of the ligand to a folding structure in a low dielectric constant solvent. Recently, the difference in the local environment of the Fe_4S_4 clusters between ferredoxin and the high-potential iron protein has been discussed.[7]

The biological important Fe_4S_4 cluster is also involved in the active site of aconitase although the Fe ion functioning as the catalytic active site does not have Cys ligation.[8,9] The catalytic activity of ferredoxin model complexes has been demonstrated in the reduction[10] and oxidation[11] of various organic substrates.

The main purpose of this study is to synthesize *P. aerogenes* ferredoxin model complexes whose reduction potentials are controlled by NH---S hydrogen bonds at ambient temperature and further to estimate the quantitative contribution of NH---S hydrogen bonds to its reduction potential. The sequence Z-Cys-Gly-NHC_6H_4-*p*-X was chosen in order to change the electronic property of the NH group of the anilide part to enhance the NH---S hydrogen bonding systematically.

Experimental Section

Preparation of Peptides. (*tert*-Butyloxycarbonyl)glycyl-*p*-fluoroanilide. An acetonitrile solution of (*tert*-butyloxycarbonyl)glycine (0.05 mol) was mixed with an acetonitrile solution of *p*-fluoroaniline (0.05 mol) by stirring at −10 °C. To the solution was added triethylamine (0.05 mol) and isobutyl chloroformate (0.05 mol) with vigorous stirring at −20 °C. The solution was allowed to stand at room temperature overnight after being stirred for 3 h at −15 °C. The solution was concentrated under reduced pressure, and ethyl acetate was added to the residue. The solution was successively washed with 2% aqueous HCl, water, 4% aqueous $NaHCO_3$, and water. After washing, the solution was dried over anhydrous Na_2SO_4. Recrystallization was performed from ethyl acetate/ether: yield 8.2 g (61%); mp 173–176 °C. Anal. Calcd for $C_{13}H_{17}N_2O_3F$: C, 58.20; H, 6.39; N, 10.44. Found: C, 58.17; H, 6.35; N, 10.38.

***N*-(Benzyloxycarbonyl)-*S*-(acetamidomethyl)-L-cysteinylglycyl-*p*-fluoroanilide (Z-Cys(Acm)-Gly-NHC_6H_4-*p*-F).** A DMF solution of glycyl-*p*-fluoroanilide hydrochloride (0.02 mol) was mixed with a DMF solution of *N*-(benzyloxycarbonyl)-*S*-(acetamidomethyl)-L-cysteine (0.02 mol) by vigorous stirring at −10 °C. To the solution was added 1-ethyl-3-(3-(dimethylamino)propyl)carbodiimide at 0 °C. The solution was neutralized with *N*-methylmorpholine and stirred overnight at room temperature. The solution was concentrated under reduced pressure. To the residue was added saturated aqueous NaCl. The products were extracted with ethyl acetate and washed successively with 2% aqueous HCl, water, 4% aqueous $NaHCO_3$, and water. After concentration under reduced pressure, the residue obtained was recrystallized from methanol–ether: yield 5.5 g (58%); mp 171–173 °C; $[\alpha]^{25}_D$ −13.6° (*c* 0.500, CH_3OH). Anal. Calcd for $C_{22}H_{25}N_4O_5SF$: C, 55.45; H, 5.29; N, 11.76. Found: C, 55.70; H, 5.57; N, 11.57.

Other *N*-(benzyloxycarbonyl)-*S*-(acetamidomethyl)-L-cysteinylglycyl-NHC_6H_4-*p*-X compounds were prepared by the same method.

Z-Cys(Acm)-Gly-NHC_6H_4-*p*-MeO: yield 5.9 g (60%); mp 198–201 °C; $[\alpha]^{25}_D$ −13.3° (*c* 0.500, CH_3OH). Anal. Calcd for $C_{21}H_{25}N_3O_5S$: C, 56.54; H, 5.78; N, 11.47. Found: C, 56.37; H, 5.82; N, 11.52.

Z-Cys-(Acm)-Gly-NHC_6H_5: yield 4.8 g (52%); mp 168–170 °C; $[\alpha]^{25}_D$ −6.9° (*c* 0.500, CH_3OH). Anal. Calcd for $C_{22}H_{26}N_4O_5S$: C, 57.63; H, 5.71; N, 12.22. Found: C, 57.51; H, 5.66; N, 12.35.

Z-Cys(Acm)-Gly-NHC_6H_4-*p*-Cl: yield 5.2 g (53%); mp 196–198 °C; $[\alpha]^{25}_D$ −11.6° (*c* 0.500, CH_3OH). Anal. Calcd for $C_{22}H_{25}N_4O_5ClS$: C, 53.60; H, 5.11; N, 11.36. Found: C, 53.58; H, 5.20; N, 11.20.

Z-Cys(Acm)-Gly-NHC_6H_4-*p*-CN: yield 4.5 g (46%); mp 195–197 °C; $[\alpha]^{25}_D$ −9.10° (*c* 0.500, CH_3OH). Anal. Calcd for $C_{23}H_{25}N_2O_5S$: C, 57.13; H, 5.21; N, 14.48. Found: C, 56.63; H, 5.25; N, 14.40.

Mercury(II) Peptide Complexes. To a DMF solution of the corresponding peptide (0.01 mol) was added $HgCl_2$ (0.02 mol). The solution was allowed to stand overnight at room temperature. A small amount of water was added to the solution, giving a white solid which was collected by filtration, washed with water, and dried over P_2O_5 in vacuo.

Synthesis of SH-Deprotected Peptides. A Hg(II) peptide complex (0.008 mol) was dissolved in 50 mL of DMF. Hydrogen sulfide gas was bubbled into the solution for 30 min at room temperature, giving black precipitates. After filtration of the precipitates, the filtrate was concentrated under reduced pressure to give a white solid. The crude peptide was recrystallized from methanol–ether. The determination of SH group in these peptides was carried out by a spectroscopic titration with 2,2'-dithiobis(5-nitropyridine).[12]

Preparation of $(Fe_4S_4)^{2+}$ Complexes. All of $(Fe_4S_4)^{2+}$ complexes with Cys-containing peptides were prepared from $[(n\text{-}Bu)_4N]_2[Fe_4S_4(S\text{-}t\text{-}Bu)_4]$ by the ligand-exchange method.[2,13,14] $[Et_4N]_2[Fe_4S_4(SPh)_4]$ and $[Et_4N]_2[Fe_4S_4(SR)_4]$ (R = Et, *i*-Pr, *i*-Bu, CH_2Ph, CH_2CH_2Ph) were prepared by the method reported by Averill et al.[15]

$[(n\text{-}Bu)_4N]_2[Fe_4S_4(Z\text{-cys-Gly-}NHC_6H_4\text{-}p\text{-}X)_4]$. $[(n\text{-}Bu)_4N]_2[Fe_4S_4(S\text{-}t\text{-}Bu)_4]$ (10^{-2} mmol) and Z-Cys-Gly-NHC_6H_4-*p*-X (4.8×10^{-2} mmol) were reacted in CH_2Cl_2 at room temperature for 15 min. The solution was concentrated under reduced pressure and a black solid was obtained and washed with 20 mL of degassed ether. The purity of the complexes was determined by the titration with thiophenol using the method reported by Gillum et al.[16] and by the ratio of ^1H NMR peak integrals of methylene protons in the Z group and $(NEt_4)^+$ protons.

Physical Measurements. All operations of physical measurements were performed under an argon atmosphere. ^1H NMR spectra were recorded on a Jeol GX-500 spectrometer. Visible spectra were obtained by using a cell of 1-mm path length on a JASCO UVDEC-5A spectrometer. Infrared spectra were recorded on a JASCO DS-402G spectrophotometer with 0.11-mm cell path of KBr. Electrochemical measurements were carried out on a YANACO P8-CV instrument with a three-electrode system. The working electrode was of glassy carbon. A saturated calomel electrode was used as a reference for potential measurements. Solutions were 2 mM in samples and 100 mM in $[(n\text{-}Bu)_4N]ClO_4$ as a supporting electrolyte. Solvents were distilled, dried over activated Linde 4A molecular sieves, degassed, and stored under an argon atmosphere.

Table I. Absorption Maxima of $[Fe_4S_4(Z\text{-cys-Gly-}NHC_6H_4\text{-}p\text{-}X)_4]^{2-}$ in CH_2Cl_2

X	abs max, nm (ϵ, M^{-1} cm^{-1})	X	abs max, nm (ϵ, M^{-1} cm^{-1})
MeO	400 (18 200)	Cl	401 (18 900)
H	402 (17 000)	CN	400 (17 900)
F	403 (17 000)		

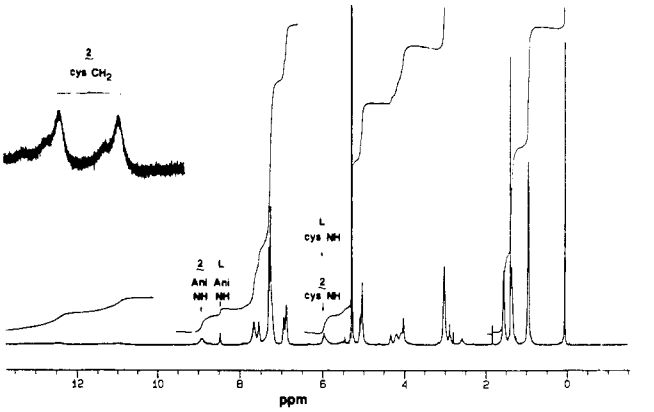

Figure 1. ^1H NMR spectrum (500 MHz) of $[(n\text{-}Bu)_4N]_2[Fe_4S_4(Z\text{-cys-Gly-}NHC_6H_4\text{-}p\text{-}F)_4]$ in CD_2Cl_2 at 303 K.

Results and Discussion

The ligands used in this study possess the sequence containing a para-substituted anilide residue in place of an Ala residue in

(7) Backes, G.; Mino, Y.; Loehr, T. M.; Meyer, T. E.; Cusanovich, M. A.; Sweeney, W. V.; Adman, E. T.; Sanders-Loehr, J. *J. Am. Chem. Soc.* **1991**, *113*, 2055.
(8) Emptage, M. H.; Kent, T. A.; Kennedy, M. C.; Beinert, H.; Münck, H. *Proc. Natl. Acad. Sci. U.S.A.* **1983**, *80*, 4674.
(9) Robbins, A. H.; Stout, C. D. *Proc. Natl. Acad. Sci. U.S.A.* **1989**, *86*, 3639.
(10) (a) Inoue, H.; Suzuki, M.; Fujimoto, N. *J. Org. Chem.* **1979**, *44*, 1722. (b) Itoh, T.; Nagano, T.; Hirobe, M. *Tetrahedron Lett.* **1980**, *21*, 1343. (c) Nakamura, A.; Kamada, M.; Sugihashi, K.; Otsuka, S. *J. Mol. Catal.* **1980**, *88*, 353.
(11) Ueyama, N.; Sugawara, T.; Kajiwara, A.; Nakamura, A. *J. Chem. Soc., Chem. Commun.* **1986**, 434.
(12) Swatditat, A.; Tsen, C. C. *Anal. Chem.* **1972**, *45*, 349.
(13) Que, L., Jr.; Anglin, J. R.; Bobrik, M. A.; Davison, A.; Holm, R. H. *J. Am. Chem. Soc.* **1974**, *96*, 6042.
(14) Bobrik, M. A.; Que, L., Jr.; Holm, R. H. *J. Am. Chem. Soc.* **1974**, *96*, 285.
(15) Averill, B. A.; Hersovitz, T.; Holm, R. H.; Ibers, J. A. *J. Am. Chem. Soc.* **1973**, *95*, 3523.
(16) Gillum, W. O.; Mortenson, L. E.; Chen, J.-E.; Holm, R. H. *J. Am. Chem. Soc.* **1977**, *99*, 584.

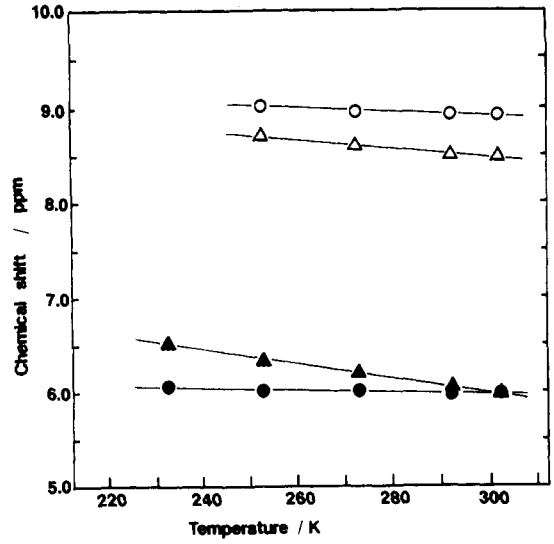

Figure 2. Temperature dependence of the chemical shifts of amide protons in $[(n\text{-}Bu)_4N]_2[Fe_4S_4(Z\text{-}cys\text{-}Gly\text{-}NHC_6H_4\text{-}p\text{-}F)_4]$ and in Z-cys-Gly-NHC_6H_4-p-F in CD_2Cl_2: (○) anilide amide proton of the complex; (△) anilide amide proton in the peptide; (●) Cys amide proton in the complex; (▲) Cys amide proton in the peptide.

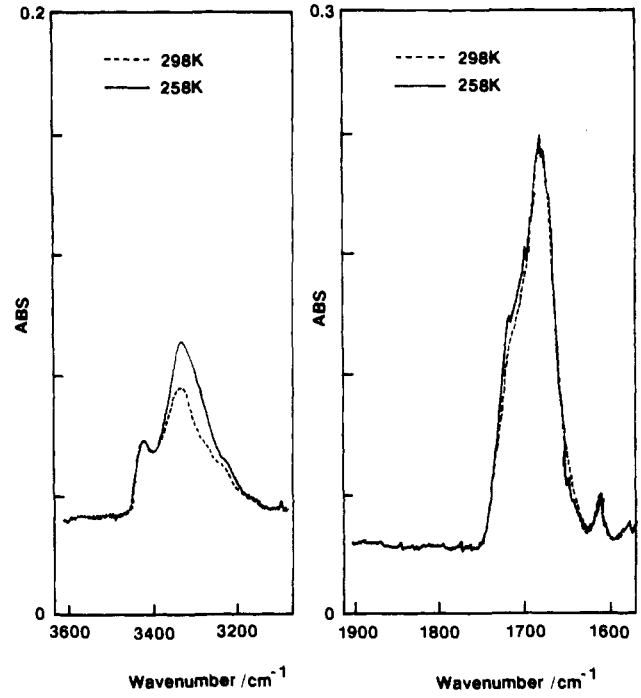

Figure 3. Temperature dependence of partial IR spectra of $[(n\text{-}Bu)_4N]_2[Fe_4S_4(Z\text{-}cys\text{-}Gly\text{-}NHC_6H_4\text{-}p\text{-}F)_4]$ in CH_2Cl_2.

the characteristic Cys-Gly-Ala sequence of *P. aerogenes* ferredoxin. Among the $(Fe_4S_4)^{2+}$ complexes with Z-Cys-Gly-NHC_6H_4-p-X ligands, $[(n\text{-}Bu)_4N]_2[Fe_4S_4(Z\text{-}cys\text{-}Gly\text{-}NHC_6H_4\text{-}p\text{-}F)_4]$ (**2**) was mainly investigated because of its advantage of being able to undergo facile ligand-exchange reactions and its thermodynamical stability. Physical measurements were generally carried out in CH_2Cl_2, having a low dielectric constant in consideration of a hydrophobic environment around the Fe_4S_4 core of *P. aerogenes* ferredoxin.

Absorption and NMR Spectra. The absorption spectra of $[(n\text{-}Bu)_4N]_2[Fe_4S_4(Z\text{-}cys\text{-}Gly\text{-}NHC_6H_4\text{-}p\text{-}X)_4]$ were measured in CH_2Cl_2 to ensure the retention of a Fe_4S_4 core (Table I). The visible absorption maxima are observed around 400 nm in CH_2Cl_2 independent of the substituents. Observed absorption maxima coincide with those of $[Fe_4S_4(Z\text{-}cys\text{-}Gly\text{-}Ala\text{-}OMe)_4]^{2-}$ and $[Fe_4S_4(Z\text{-}cys\text{-}Gly\text{-}Ala\text{-}cys\text{-}OMe)_2]^{2-}$.[5] The result indicates that all the complexes prepared have the $(Fe_4S_4)^{2+}$ core.

Figure 1 shows the ^1H NMR spectrum (500 MHz) of **2** in CD_2Cl_2 at 303 K as a representative of the complexes prepared. The resonances of side-chain CH_2 protons of the Cys residue are observed at 12.4 and 11.0 ppm contact-shifted through the H–C–S–Fe bonds by the $(Fe_4S_4)^{2+}$ core. In addition, those signals were temperature-dependent (11.7 and 10.3 ppm at 273 K). The contact shifts of Cys CH_2 protons were reported for many $(Fe_4S_4)^{2+}$ complexes such as $[Fe_4S_4(Ac\text{-}cys\text{-}NHMe)_4]^{2-}$,[13] $[Fe_4S_4(12\text{-peptides})_4]^{2-}$ (12-peptides = *t*-Boc(-Gly-Cys-Gly-)$_4NH_2$[13] (*t*-Boc = *tert*-butoxycarbonyl), $[Fe_4S_4(Z\text{-}cys\text{-}Gly\text{-}Ala\text{-}OMe)_4]^{2-}$, and $[Fe_4S_4(Z\text{-}cys\text{-}Gly\text{-}Ala\text{-}cys\text{-}OMe)_2]^{2-}$.[5] The contact shift of Cys CH_2 protons of **2** indicates coordination of the cysteine thiolato to a Fe_4S_4 core. The assignment of the Cys CH proton observed at 4.3 ppm was carried out by detection of vicinal coupling with Cys NH proton and, furthermore, confirmed by the 2D H–H COSY method.

We examined the ^1H NMR spectrum of **2** in the presence of an excess of the Z-Cys-Gly-NHC_6H_4-p-F ligand in CD_2Cl_2 as shown in Figure 1. The amide NH signals were confirmed by their disappearance on addition of 4 equiv of CD_3OD in the solution. Two NH signals observed at 8.9 (line width 32 Hz) and 8.5 ppm (line width 8 Hz) were assigned to anilide NH of **2** and anilide NH of the SH-deprotected peptide, respectively. A broad signal at 5.9 ppm was assigned to the overlapped peaks of two slow-exchanging protons of Cys NH of **2** and of the SH-deprotected peptide.

Figure 2 shows the temperature dependence of amide NH signals for **2** and the SH-deprotected peptide. The broad Cys NH signal at 303 K separates into a sharp signal and a broad signal at lower temperature. A large temperature dependence of the two sharp signals was observed for anilide NH and Cys NH of the SH-free peptide, while it is small for the broad signals of anilide NH and Cys NH in **2**. The observed broadness (line width 32 Hz) may be attributed to the slight paramagnetic character from the $(Fe_4S_4)^{2+}$ core because the peptide NH signal usually exhibits a peak width of 7–14 Hz even with large J_{HN_α} values. Signals due to Gly NH protons of unreacted and reacted ligands appear to be overlapped with phenyl protons of the Z residues. The assignment of Gly NH in **2** was established by the observations of the vicinal coupling with Gly CH_2 and their correlation in the 2D H–H COSY spectrum.

The anilide NH proton of the ligand in **2** resonates at a lower magnetic field than that of the unreacted peptide. On the other hand, the Cys NH proton of the ligand in **2** resonates at a higher magnetic field than that of the unreacted peptide. This suggests that intramolecular NH---S hydrogen bonds from anilide NH to the S atom of a Cys residue are formed in the complex, although the resonance position of the NH signal reflects the strength of not only intramolecular hydrogen bonds[17] but also solvation. Slowly exchangeable NH protons in *Clostridium acidi-urici* ferredoxin have been reported to exhibit ^1H NMR signals at 9.2 and 7.8 ppm,[18] which are close to the chemical shift of the broad hydrogen-bonded anilide NH protons of **2**. Thus, little isotropic shift of amide NH through the NH---S hydrogen bond is found in the $[Fe_4S_4(SR)_4]^{2-}$ state.

Infrared Spectra. Figure 3 shows the IR spectra of **2** in CH_2Cl_2 at 298 and 253 K. Bystrov et al. have studied a terminal-blocked dipeptide containing the Ala-Ala sequence in dilute CCl_4 solution.[19] Among two NH stretchings (3420 and 3340 cm^{-1}), the low-frequency band was assigned to the intra- and intermolecular hydrogen-bonded NH groups and the high-frequency band to groups not forming such bonds. In the present case, the strong NH band at 3330 cm^{-1} indicates that most of the NH groups are involved in interaction with donor atoms forming the NH---O=C and NH---S bonds. The NH band of **2** at 3330 cm^{-1} was strengthened

(17) Gierasch, L. M.; Rockwell, A. L.; Thompson, K. F.; Briggs, M. S. *Biopolymers* **1985**, *24*, 117.
(18) Packer, E. L.; Sweeney, W. V.; Thompson, K. F.; Sternlicht, H.; Shaw, E. N. *J. Biol. Chem.* **1977**, *252*, 2245.
(19) Bystrov, V. F.; Portnova, S. L.; Tsetlin, V. I.; Ivanov, V. T.; Ovchinnikov, Y. A. *Tetrahedron* **1969**, *25*, 493.

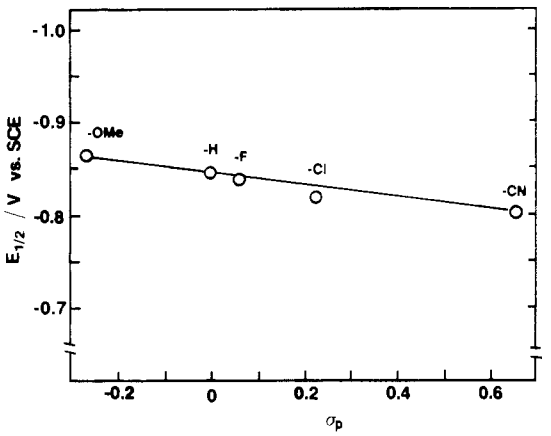

Figure 4. Correlation of the reduction potentials of $[(n\text{-}Bu)_4N]_2[Fe_4S_4(Z\text{-cys-Gly-NHC}_6H_4\text{-}p\text{-}X)_4]$ with Hammett σ_p constants in CH_2Cl_2 at 298 K.

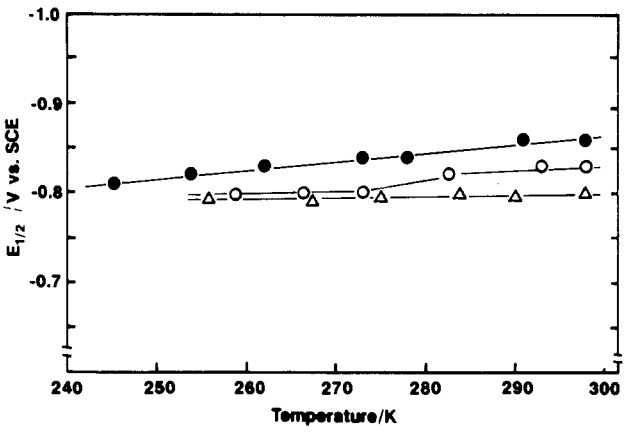

Figure 5. Temperature dependence of reduction potentials of $[(n\text{-}Bu)_4N]_2[Fe_4S_4(Z\text{-cys-Gly-NHC}_6H_4\text{-}p\text{-}X)_4]$ in CH_2Cl_2: (○) *p*-MeO; (●) *p*-F; (△) *p*-CN.

at lower temperature, whereas the CO bonds in a region of 1670–1750 cm^{-1} were unchanged. The result suggests that the band at 3330 cm^{-1} arises from the NH groups involved in the formation of NH---S bonds.

Redox Properties. The electrochemical reduction of $[Fe_4S_4(Z\text{-cys-Gly-NHC}_6H_4\text{-}p\text{-}X)_4]^{2-}$ was examined by cyclic voltammetry. Our electrochemical measurement of **2** in CH_2Cl_2 at 298 K afforded a 3−/2− redox couple with good reversibility. The reduction potential was observed at −0.83 V vs SCE, which was far more positive than those of $(Fe_4S_4)^{2+}$ complexes with alkane- and arenethiolato ligands.[20] The results in the reversibilities of the 3−/2− redox couple for these complexes indicate that the complex having a stronger electron-withdrawing para-substituted anilide ligand exhibits a larger i_{pc}/i_{pa} value, e.g. 1.0 for **2** and 0.9 for $[Fe_4S_4(Z\text{-cys-Gly-NHC}_6H_4\text{-}p\text{-OMe})_4]^{2-}$. In addition, further reduction of the peptide complex provided a 4−/3− redox couple, though its reversibility was not as good as above.

The electrochemical reduction was examined for $[Fe_4S_4(SPh)_4]^{2-}$ in CH_2Cl_2 to clarify the solvent effect on the reduction of $(Fe_4S_4)^{2+}$ complexes. The reduction of $[Fe_4S_4(SPh)_4]^{2-}$ provided an irreversible 3−/2− redox couple. The further reduction leads to multielectron reduction. Contrary to our results, DePamphilis et al. reported that the electrochemical reduction of $[Fe_4S_4(SPh)_4]^{2-}$ in DMF gave a 3−/2− redox couple with good reversibility as well as a 4−/3− redox couple with fairly good reversibility.[3] The discrepancy would arise from the solvent used. The reduction product of $[Fe_4S_4(SPh)_4]^{2-}$ appears to be stabilized in polar DMF by solvation. The unique stability of the reduced state of **2** even in nonpolar CH_2Cl_2 is thus caused by a Z-cys-Gly-NHC_6H_4-*p*-F ligand. Furthermore, the stabilization of the reduced state would raise the reduction potential to the positive side.

In order to clarify the influence of thiolate ligands on the reduction potential of **2**, the correlation of reduction potentials of $[Fe_4S_4(Z\text{-cys-Gly-NHC}_6H_4\text{-}p\text{-}X)_4]^{2-}$ with the Hammett σ_p constant for aromatic substituents was examined in CH_2Cl_2 at 298 K (Figure 4). These ligands were found to exert an influence on the reduction potential. Potentials were linearly related to the Hammett *p* constant, with the most positive potential found for **1** (−0.80 V vs SCE). The observed behavior of the reduction potential is most reasonably related to the amounts of NH---S hydrogen bonds between the S atom of a Cys residue and the amide NH of an anilide residue. The amide NH proton whose protonic character is enhanced by an electron-withdrawing aryl group tends to form a more stable NH---S hydrogen bond. In other words, amide NH protons of anilide residues with an electron-withdrawing para substituent are expected to form larger amounts of hydrogen bonds.

The temperature dependence of the reduction potentials of $[Fe_4S_4(Z\text{-cys-Gly-NHC}_6H_4\text{-}p\text{-}X)_4]^{2-}$ was examined in CH_2Cl_2 to clarify the relationship between the reduction potential and amounts of NH---S hydrogen bonds in more detail (Figure 5). The reduction potentials slightly shifted to the positive side as the temperature was lowered. However, the temperature dependence of the reduction potential became smaller as the electron-withdrawing tendency of the substituent increased. Especially, the reduction potential of **1** remained constant in spite of the temperature variation. Finally, the reduction potentials of all complexes approached −0.80 V vs SCE at lower temperatures. This behavior of the reduction potential is explained by the amounts of NH---S hydrogen bonds. The anilide NH which has not participated in the formation of NH---S hydrogen bonds at 298 K would make hydrogen bonds due to the conformational freezing of a conformer containing a NH---S bond at lower temperature. The conformer of the peptide ligand probably has a structure closely similar to the β-II hairpin turn as proposed in Figure 6. This is consistent with the foregoing observation that the NH bond at 3330 cm^{-1} was strengthened at lower temperature. Such conformational freezing was observed in $[Fe_4S_4(Z\text{-cys-Gly-Ala-OMe})_4]^{2-}$ and $[Fe_4S_4(Z\text{-cys-Gly-Ala-cys-OMe})_2]^{2-}$ complexes.[5] $[Fe_4S_4(Z\text{-cys-Gly-NHC}_6H_4\text{-}p\text{-}X)_4]^{2-}$ complexes exhibited the same reduction potential independent of the substituents, when all of anilide NH took part in the formation of NH---S hydrogen bonds.

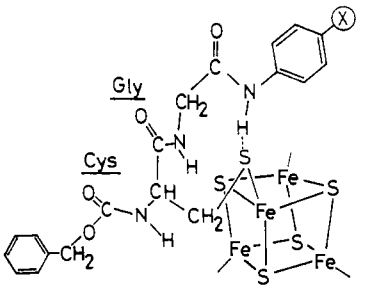

Figure 6. Proposed structure having NH---S hydrogen bonds in $[Fe_4S_4(Z\text{-cys-Gly-NHC}_6H_4\text{-}p\text{-}X)_4]^{2-}$.

The NH---S hydrogen bonds appear to stabilize the reduced state of $[Fe_4S_4(Z\text{-cys-Gly-NHC}_6H_4\text{-}p\text{-}X)_4]^{2-}$ and raise their redox potential to the positive side as a result. NH---S hydrogen bonds seems to delocalize the negative charge on the thiolato ligand. Upon reduction of $[Fe_4S_4(Z\text{-cys-Gly-NHC}_6H_4\text{-}p\text{-}X)_4]^{2-}$, the excessive negative charge would delocalize to the H atom through the S---H bond. Carter et al. reported that the N to S distance for the NH---S contact was shortened upon reduction of oxidized high-potential iron protein.[21] Such shortening is advantageous to the delocalization of negative charge. Unfortunately, the X-ray analysis of the reduced ferredoxin has not been carried out because of its extreme instability.

(20) Cambray, J.; Lane, R. W.; Wedd, A. G.; Johnson, R. W.; Holm, R. H. *Inorg. Chem.* **1977**, *6*, 2565.

(21) Carter, C. W., Jr.; Kraut, J.; Freer, S. T.; Alden, R. A. *J. Biol. Chem.* **1974**, *249*, 6339.

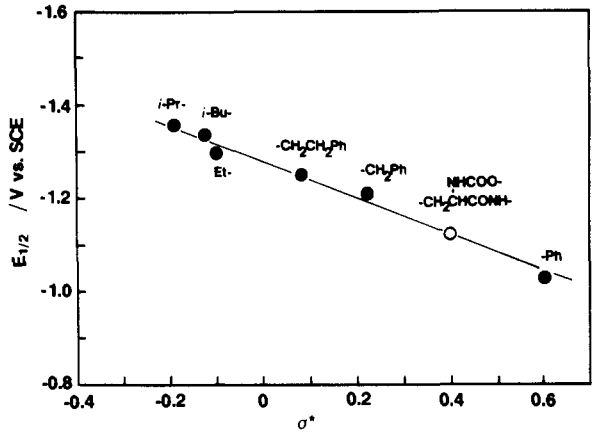

Figure 7. Correlation of the reduction potentials of $[Et_4N]_2[Fe_4S_4(SR)_4]$ with Taft σ^* constants in CH_2Cl_2 at 298 K.

Contribution of NH---S Hydrogen Bonds to the Reduction Potential. Among the present complexes, **1** is the most interesting one as a *P. aerogenes* ferredoxin model, because all of its anilide NH groups participate in NH---S hydrogen bonds at ambient temperature. Therefore, it is useful for clarification of the contribution of NH---S hydrogen bonds to its reduction potential. The direct electronic contribution by the Cys thiolate ligand to the redox potential of **1** should be considered because the electronic property apparently exerts an influence on the reduction potential of the $(Fe_4S_4)^{2+}$ complex.[3] The direct electronic contribution in the Cys-containing oligopeptide $(Fe_4S_4)^{2+}$ complex has been discussed in terms of the Cys thiolate, whose Taft σ^* value is 0.40.[22]

Figure 7 shows the correlation of reduction potentials of known $(Fe_4S_4)^{2+}$ complexes having alkanethiolato ligands with the Taft σ^* constant. From the figure, the expected reduction potential of **1** is ca −1.13 V vs SCE on the basis of the σ^* value (0.40) for a $CH_2CH(NHCOO-)CONH$ group. The contribution of NH---S hydrogen bonds to the reduction potential is calculated to be 0.33 V by subtracting the potential regulated by the electronic property of a ligand (−1.13 V vs SCE) from the observed potential (−0.80 V vs SCE in CH_2Cl_2).

The $(Fe_4S_4)^{2+}$ core of *P. aerogenes* ferredoxin is surrounded by a number of hydrophobic side chains of amino acid residues such as Ile, Val, and Ala. Thus, the reduction potential of **1** in CH_2Cl_2 is not consistent with the usual trend of the positive shift with increase of the dielectric constant of solvent. Actually, Depamphilis et al. have reported that the reduction potential of the $(Fe_4S_4)^{2+}$ complex markedly shifted to the positive side in the order Me_2SO–H_2O > Me_2SO > DMF.[3] Therefore, the effect of solvents with low dielectric constants such as CH_2Cl_2, etc. on the redox potential was examined. The observed redox potential of $(NEt_4)_2[Fe_4S_4(SPh)_4]$ was observed at −1.0 V vs SCE in CH_2Cl_2 (dielectric constant 8.93), −1.1 V in isobutyronitrile (20.4), −1.0 V in acetonitrile (37.5), and −1.0 V in DMF (36.7). Thus, these solvents exerted little influence on the reduction potential of the $(Fe_4S_4)^{2+}$ complexes examined. The present results lead to the conclusion that the reduction potential of **1** in CH_2Cl_2 is applicable to *P. aerogenes* ferredoxin. In other words, the hydrophobic amino acid side chains around the $(Fe_4S_4)^{2+}$ core in the active site of native bacterial ferredoxins form a low dielectric constant environment as in CH_2Cl_2 which stabilizes the NH---S hydrogen bond from the peptide backbone chain to the Cys sulfur atom.

On the basis of X-ray analysis, Adman et al. has proposed the existence of NH---S* (S* = inorganic sulfide) hydrogen bonds from the peptide backbone chain to the inorganic sulfur atoms of $(Fe_4S_4)^{2+}$ core in ferredoxins.[23] Our results on the contribution of this type of NH---S* hydrogen bond to the reduction potential of the $(Fe_4S_4)^{2+}$ complex will be published elsewhere.

Recent detailed study of various ferredoxins using the X-ray crystallographic and resonance Raman analyses has suggested that the variation in the reduction potentials is due to difference in the local environments of the clusters.[7] Of course, the effect of dielectric constant around the cluster is significant for changing the reduction potential as has been theoretically pointed out by Kassner and Young.[24] Our results emphasize that the peptide chain constructs a heterogeneous environment having the NH---S hydrogen bond (strong solvation to the cluster) strengthened by a low dielectric constant environment as with a nonpolar solvent. However, further study will be required because other factors, e.g. distortion of the cluster derived by the peptide ligation, could possibly influence the positive shift.

Summary

The reduction potential of $[Fe_4S_4(Z\text{-cys-Gly-NHC}_6H_4\text{-}p\text{-X})_4]^{2-}$ was controlled by not only the electronic property of the thiolate ligand but also the intramolecular NH---S hydrogen bonds from amide NH of an anilide residue probably to the cysteinyl sulfur atom. The formation of NH---S hydrogen bonds arises from the amide NH proton, whose cationic character was enhanced by an electron-withdrawing para-substituted aryl group. Especially, amide NH protons of anilide residues with an electron-withdrawing substituent at a para position formed larger amount of hydrogen bonds. The most positive potential was observed at −0.80 V vs SCE for $[Fe_4S_4(Z\text{-cys-Gly-NHC}_6H_4\text{-}p\text{-CN})_4]^{2-}$, in which all of the amide NH groups of an anilide residue participated in intramolecular NH---S hydrogen bonds. Its reduction potential controlled by the direct electronic property of the thiolate ligand and the effect of NH---S hydrogen bonds on the Fe–S bond could be estimated to be −1.13 V vs SCE and 0.33 V, respectively, in our synthetic peptide model complexes.

Our present finding seems to be important for understanding the influence of polypeptides on the electron-transfer function of ferredoxins.

(22) Ohno, R.; Ueyama, N.; Nakamura, A. *Inorg. Chim. Acta* **1990**, *169*, 253.

(23) Adman, E. T.; Watenpaugh, K. D.; Jensen, L. H. *Proc. Natl. Acad. Sci. U.S.A.* **1975**, *72*, 4854.

(24) Kassner, R. J.; Young, W. *J. Am. Chem. Soc.* **1977**, *99*, 4351.